Inorganic Chemistry
Article

Inorg. Chem. **2010**, *49*, 3305–3309 **3305**
DOI: 10.1021/ic9022739

Sacrificial Template Method for Fabrication of Submicrometer-Sized $YPO_4:Eu^{3+}$ Hierarchical Hollow Spheres

Lihui Zhang, Guang Jia, Hongpeng You,* Kai Liu, Mei Yang, Yanhua Song, Yuhua Zheng, Yeju Huang, Ning Guo, and Hongjie Zhang*

State Key Laboratory of Rare Earth Resource Utilization, Changchun Institute of Applied Chemistry, Chinese Academy of Sciences, Changchun, 130022 and Graduate University of the Chinese Academy of Sciences, Beijing 100049, P. R. China

Received November 17, 2009

Large-scale good-quality submicrometer-sized $YPO_4:Eu^{3+}$ hollow spheres were synthesized by utilizing the colloidal spheres of $Y(OH)CO_3:Eu^{3+}$ as a sacrificial template and $NH_4H_2PO_4$ as a phosphorus source, for the first time. The whole process mainly consists of the hydrothermal reaction and acid erosion. The $YPO_4:Eu^{3+}@Y(OH)CO_3:Eu^{3+}$ core−shell structures were first obtained after the hydrothermal process. Then, the remaining $Y(OH)CO_3:Eu^{3+}$ was removed by selective dissolution in a dilute nitric acid solution. The $YPO_4:Eu^{3+}$ hollow spheres were characterized by X-ray diffraction (XRD), scanning electron microscopy (SEM), transmission electron microscopy (TEM), and photoluminescence (PL). The formation mechanism was also investigated. The obtained $YPO_4:Eu^{3+}$ hollow spheres may have potential applications in cell biology, drug release, and diagnosis, due to high chemical stability and luminescence functionality.

1. Introduction

The fabrication of monodisperse hollow spheres with a controllable size and shape is currently one of the fastest growing areas of materials research.[1,2] The resulting hollow nano- and microspheres are of great technological importance for their potential applications in catalysis, chromatography, protection of biologically active agents, fillers (or pigments/coatings), waste removal, and large bimolecular-release systems.[3−13] Various hollow spheres including carbons,[14] polymers,[15] metals,[16] and inorganic materials[17] have been synthesized by using spherical particles such as polystyrene beads or silica sol as a template.[18] In a typical procedure, template particles are coated in solution either by controlled surface precipitation of inorganic molecule precursors (silica, titania, etc.) or by direct surface reactions that utilize specific functional groups on the cores to create core/shell composites. The template particles are subsequently removed by selective dissolution in an appropriate solvent or by calcination at elevated temperatures in the air to generate hollow spheres.

Among the templates mentioned above, a promising sacrificial template interested us very much. That is, the template itself is involved as a reactant in the synthetic process. The resultant shell forms around the surface of the template and takes the shape of the template.[19] With the reaction proceeding, the sacrificial template is gradually consumed partially or completely during the shell-forming process.[20] The process is therefore typically more efficient, especially when the sacrificial template is completely consumed during the shell-forming process. With this method, Zhu and co-workers recently reported the preparation of CdX (X = Te, Se, S) hollow nanospheres utilizing Cd(OH)Cl nanoparticles as a sacrificial template[19] and ZnX (X = S, Se)

*To whom correspondence should be addressed. E-mail: hpyou@ciac.jl.cn (H.Y.) or hongjie@ciac.jl.cn (H.Z.).

(1) Chen, M.; Wu, L. M.; Zhou, S. X.; You, B. *Adv. Mater.* **2006**, *18*, 801.
(2) Jia, G.; Yang, M.; Song, Y. H.; You, H.; Zhang, H. *Cryst. Growth Des.* **2009**, *9*, 301.
(3) Jiang, P.; Bertone, J. F.; Colvin, V. L. *Science* **2001**, *291*, 453.
(4) Kidambi, S.; Dai, J. H.; Bruening, M. L. *J. Am. Chem. Soc.* **2004**, *126*, 2658.
(5) Wang, T.; Cohen, R. E.; Rubner, M. F. *Adv. Mater.* **2002**, *14*, 1534.
(6) Wang, Y.; Cai, L.; Xia, Y. *Adv. Mater.* **2005**, *17*, 473.
(7) Wang, Y.; Xia, Y. *Nano. Lett.* **2004**, *4*, 2047.
(8) Caruso, F. *Adv. Mater.* **2001**, *13*, 11.
(9) Xu, X.; Asher, S. A. *J. Am. Chem. Soc.* **2004**, *126*, 7940.
(10) Yang, Z.; Nui, Z.; Lu, Y.; Hu, Z.; Han, C. C. *Angew. Chem., Int. Ed.* **2003**, *42*, 1943.
(11) Kim, J.; Yoon, S.; Yu, J. *Chem. Commun.* **2003**, 790.
(12) Li, Y.; Shi, J.; Hua, Z.; Chen, H.; Ruan, M.; Yan, D. *Nano. Lett.* **2003**, *3*, 609.
(13) Caruso, F.; Caruso, R. A.; Mohwald, H. *Science* **1998**, *282*, 1111.
(14) Lee, J.; Sohn, K.; Hyeon, T. *J. Am. Chem. Soc.* **2001**, *123*, 5146.
(15) Donath, E.; Sukhorukov, G. B.; Caruso, F.; Davis, S. A.; Mohwald, H. *Angew. Chem., Int. Ed.* **1998**, *37*, 2202.
(16) Egan, G. L.; Yu, J.-S.; Kim, C. H.; Lee, S. J.; Schaak, R. E.; Mallouk, T. E. *Adv. Mater.* **2000**, *12*, 1040.
(17) Imhof, A. *Langmuir* **2001**, *17*, 3579.
(18) Han, S.; Sohn, K.; Hyeon, T. *Chem. Mater.* **2001**, *12*, 333.
(19) Miao, J. J.; Jiang, L. P.; Liu, C.; Zhu, J. M.; Zhu, J. J. *Inorg. Chem.* **2007**, *46*, 5673.
(20) Lou, X. W.; Yang, Z. C. *Adv. Mater.* **2008**, *20*, 3987.

© 2010 American Chemical Society
Published on Web 03/02/2010

hollow spheres based on ZnO nanospheres,[21] and Huang et al. reported the synthesis of Cu_2O hollow spheres from Cu nanospheres and so on.[22] These reports were focused on oxide, sulphide, nitride, and so on. However, reports on salts were limited.

As we know, yttrium orthophosphate crystallizes with the zircon structure (xenotime type) with a tetragonal symmetry ($a = b = 6.822$ and $c = 6.018$ Å) and space group I_1/amd. The structure can be described as chains parallel to the c axis of corner-sharing structural units built of a (YO_8) dodecahedron and (PO_4) tetrahedron linked together by an edge. The europium orthophosphate $EuPO_4$ crystallizes with the monazite type, but partial substitution of Eu^{3+} for Y^{3+} does not affect the xenotime structure of YPO_4.[23] Since YPO_4:Eu^{3+} materials are of particular interest in the production of luminescent material, various micro/nanostructures of the Eu^{3+}-activated YPO_4 phosphors have been prepared, and their photoluminescence has been well discussed.[23−26] However, the hollow structure of YPO_4 has not been reported up to now. Herein, we describe a simple method to synthesize the YPO_4:Eu^{3+}@$Y(OH)CO_3$:Eu^{3+} core−shell structure and the hollow structure of the YPO_4:Eu^{3+} phosphors. We used the colloidal spheres of the $Y(OH)CO_3$:Eu^{3+} obtained via urea-based homogeneous precipitation as a sacrificial template. The colloidal spheres of the $Y(OH)CO_3$:Eu^{3+} partly reacted with $NH_4H_2PO_4$ to create YPO_4:Eu^{3+}@$Y(OH)CO_3$:Eu^{3+} composites in the hydrothermal process, and the remaining $Y(OH)CO_3$:Eu^{3+} was subsequently removed by selective dissolution in an appropriate nitric acid solution at room temperature to obtain the hollow structure.

2. Experimental Section

2.1. Materials. $Y_{0.95}Eu_{0.05}(NO_3)_3$ aqueous solution (1 M) was obtained by dissolving Y_2O_3 (99.99%) and Eu_2O_3 (99.99%) in HNO_3 solution under heating with agitation. All other analytical grade chemicals were purchased from Beijing Chemical Corporation and used as received without further purification.

2.2. Preparation of Monodisperse $Y(OH)CO_3$:Eu^{3+} Colloid Spheres. The monodisperse colloid spheres of $Y(OH)CO_3$:Eu^{3+} were prepared via a urea-based homogeneous precipitation process.[27] A total of 0.75 mL of $Y_{0.95}Eu_{0.05}(NO_3)_3$ (1 M) and 1.5 g of urea [$CO(NH_2)_2$] were dissolved in deionized water. The total volume of the solution was about 50 mL. The above solution was first homogenized under magnetic stirring at room temperature for 2 h. The resultant solution was then reacted at 90 °C for 2 h in the oil bath. The obtained suspension was separated by centrifugation and collected after washing with deionized water several times.

2.3. Preparation of the YPO_4:Eu^{3+}@$Y(OH)CO_3$:Eu^{3+} Core−Shell Structure and the YPO_4:Eu^{3+} Hierarchical Hollow Spheres. In a typical synthesis, the as-obtained 0.75 mmol of $Y(OH)CO_3$:Eu^{3+} precipitation was dispersed into deionized water by ultrasonic and vigorous stirring for half an hour. A total of 0.08 g of $NH_4H_2PO_4$ dissolved in a proper amount of deionized water was dripped into the dispersion followed by further stirring. A total of 0.1 g of cetyltrimethylammonium bromide (CTAB) was also added to the reaction mixture to modify the sample's structure and morphology. The reaction mixture was transferred into a 50 mL Teflon-lined autoclave and kept at 200 °C for 15 h. The obtained white products were carefully collected after washing with deionized water and alcohol and drying at 60 °C for 24 h in the air. The hollow structures were obtained after being treated by dilute nitric acid solution at room temperature for 72 h and were carefully collected.

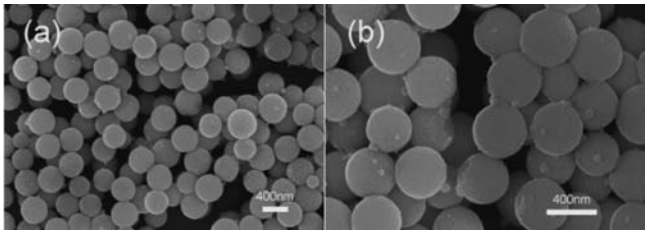

Figure 1. SEM image of the precursor of $Y(OH)CO_3$:Eu^{3+}.

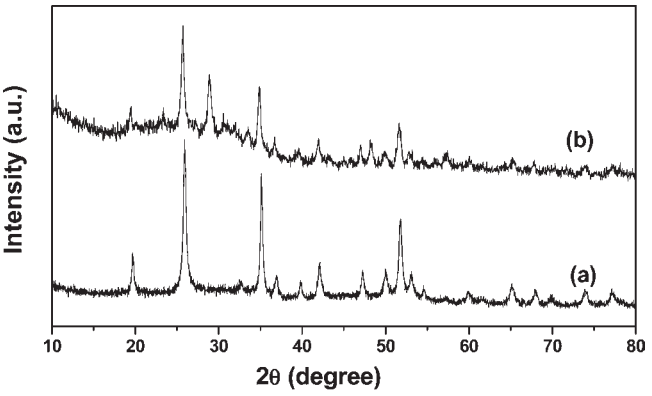

Figure 2. XRD patterns of the as-prepared samples by a hydrothermal process for 15 h without (a) and with (b) annealing at 750 °C.

2.4. Characterization. The samples were characterized by powder X-ray diffraction (XRD) performed on a D8 Focus diffractometer (Bruker). The morphology and composition of the sample were inspected using a field emission scanning electron microscope (SEM; S-4800, Hitachi; transmission electron microscopy (TEM) images and selected area electron diffraction (SAED) patterns were obtained using a TECNAI G2 transmission electron microscope operating at 200 kV. Photoluminescence (PL) excitation and emission spectra were recorded with a Hitachi F-4500 spectrophotometer equipped with a 150 W xenon lamp as the excitation source at room temperature.

3. Results and Discussion

3.1. YPO_4@$Y(OH)CO_3$ Core−Shell Structure. Figure 1 shows the SEM images of $Y(OH)CO_3$:Eu^{3+} particles synthesized by a general urea-based homogeneous precipitation method. One can see that the obtained $Y(OH)CO_3$:Eu^{3+} exhibits uniform monodisperse colloid spheres with average diameters of about 350−400 nm.

Figure 2a shows the XRD pattern of the as-prepared products $Y(OH)CO_3$ that were treated with $NH_4H_2PO_4$ at 200 °C for 15 h in the hydrothermal process. One can see that all of the diffraction peaks can be readily indexed to the crystallized tetragonal YPO_4 (JCPDS No. 11−0254), revealing the formation of a YPO_4 phase. To further determine the chemical composition of the product, the

(21) Geng, J.; Liu, B.; Xu, L.; Hu, F. N .; Zhu, J. J. *Langmuir* **2007**, *23*, 102866.
(22) Huang, J. R.; Su, D. B. *Chem.—Eur. J.* **2006**, *12*, 3805.
(23) Nedelec, M.; Avignant, D.; Mahiou, R. *Chem. Mater.* **2002**, *14*, 651.
(24) Fang, Y. P.; Xu, A. W; Song, R. Q.; Zhang, H. X.; You., L. P.; Yu, J. C.; Liu, H. Q. *J. Am. Chem. Soc.* **2003**, *125*, 16025.
(25) Li, C. X.; Hou, Z. Y.; Zhang, C. M.; Yang, P. P.; Li, G. G.; Xu, Z. H.; Fan, Y.; Lin, J. *Chem. Mater.* **2009**, *21*, 4598.
(26) Huo, Z. Y.; Chen, C.; Li, Y. D. *Chem. Commun.* **2006**, 3522.
(27) Li, J. G.; Li, X. D.; Sun, X. D.; Ishigaki, T. *J. Phys. Chem. C* **2008**, *112*, 11707.

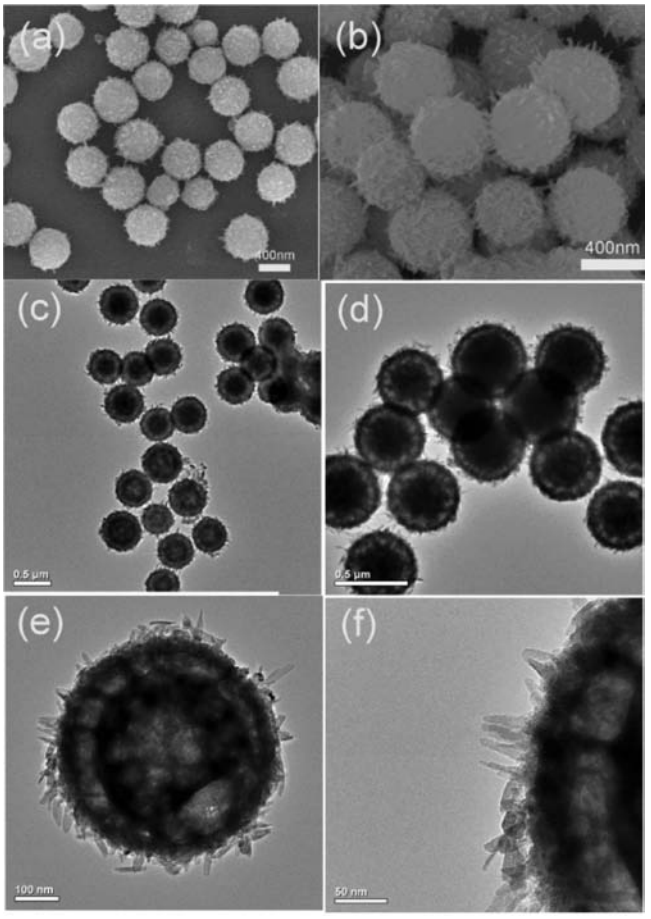

Figure 3. SEM (a, b) and TEM (c−f) images of the as-obtained sample after hydrothermal treatment.

sample was annealed at 750 °C for 2 h. The XRD pattern (Figure 2b) indicates that the peaks can be well indexed to the cubic Y_2O_3 (JCPDS No. 41−1105) except for the peaks from YPO_4. It is known that $Y(OH)CO_3$ is amorphous and cannot form the diffraction peaks under XRD excitation. Thus, only the diffraction peaks of the YPO_4 in the XRD pattern of the as-prepared sample were observed. When the sample was annealed at 750 °C, the $Y(OH)CO_3$ was thermally decomposed into Y_2O_3. Therefore, the diffraction peaks of Y_2O_3 appear. In other words, the $Y(OH)CO_3$ precursor had not been completely converted into YPO_4 after the hydrothermal process, revealing that the product is composed of YPO_4 and $Y(OH)CO_3$ after the hydrothermal treatment.

Figure 3 gives low-magnification and high-magnification SEM images of the as-obtained sample after hydrothermal treatment. One can see that the as-prepared sample consists of uniform spheres. Compared with the precursor of $Y(OH)CO_3:Eu^{3+}$, the surface of the obtained spheres becomes rough. A careful observation reveals that the rough surface is aggregates of numerous belts. At the same time, the diameters of the spheres are slightly larger than the sacrificial template (Figure 1). To clearly see the structure of the microspheres, transmission electron microscopy (TEM) was performed. Figure 3c−f show the TEM images of as-prepared samples after the hydrothermal treatment. It is noted that all the spheres have a shell about 20−30-nm-thick outside. The surface of the shell is aggregates of numerous belts, which is in agreement with the SEM image. In the center, most of the spheres have a large dark spherical zone with several tiny belts grown on it (Figure 3d). Considering the XRD results mentioned above, one can conclude that the outer shell is the as-formed YPO_4 and the large inner dark zone is the remainder of the $Y(OH)CO_3$. The tiny belts on the interior spheres are also the formed YPO_4, just as the ones growing on the exterior shell are. A double-shell, even triple-shell, structure can be obtained, which can be seen from TEM images in Figure 3c and e. But the single-shell product is predominant. These results confirm the formation of the $YPO_4:Eu^{3+}@Y(OH)CO_3:Eu^{3+}$ core−shell structure, and the colloidal spheres of $Y(OH)CO_3$ had not been completely converted into YPO_4 after the hydrothermal process.

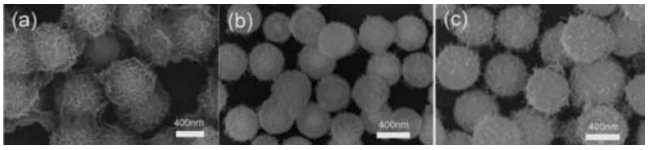

Figure 4. SEM images of the as-prepared samples prepared at (a) 100 °C, 30 h; (b) 150 °C, 30 h; (c) 200 °C, 30 h.

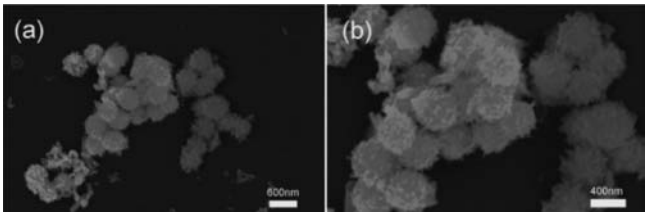

Figure 5. SEM images of the as-prepared samples prepared at 200 °C without CTAB.

In our experiments, it was found that the morphology of the as-obtained submicrosized spheres strongly depended on the reaction temperature and the addition of CTAB. Figure 4 shows the SEM images of the as-prepared samples prepared at different temperatures. When the reaction temperature was 100 °C, the obtained product consists of subspheres with the meshwork formed around them (Figure 4a). As the reaction temperature was increased, the obtained product is composed of uniform subspheres with tiny belts in the surface, which can be seen from the SEM images (Figure 4b). With the change of the temperature from 100 to 200 °C, the surface of the spheres became more and more rough (Figure 4c), due to the formation of larger belts in their surface. During the reaction process, CTAB plays an important role in the formation of the well-dispersed spherical samples. Figure 5 presents the SEM image of the as-prepared sample at a reaction temperature of 200 °C without CTAB. Compared to the samples prepared with the addition of CTAB, one can notice that single rods of YPO_4 and their self-assembly structure are present in the sample without being uniform. Therefore, CTAB might play an important role in the formation of a well-dispersed $YPO_4:Eu^{3+}@Y(OH)CO_3:Eu^{3+}$ sample in the hydrothermal process.

3.2. $YPO_4:Eu^{3+}$ Hollow Spheres. The core−shell structured composites were treated by a dilute nitric acid solution at room temperature for a proper time. Figure 6a gives the XRD pattern of the as-prepared YPO_4 sample after being treated by nitric acid. All the diffraction peaks can be

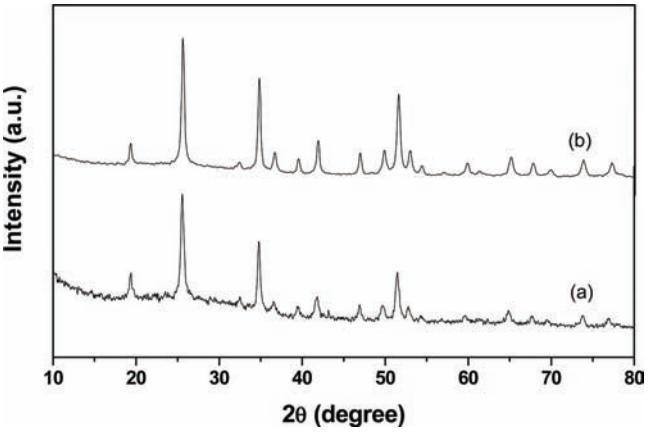

Figure 6. XRD data of the YPO_4 hollow structure obtained by treatment with nitric acid, without (a) and with (b) annealing at 750 °C.

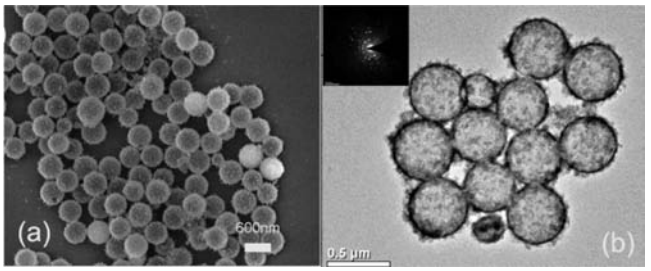

Figure 7. SEM (a) and TEM (b) images of the hollow structure YPO_4.

well indexed to the pure tetragonal phase YPO_4 (JCPDS. No. 11−0254). The obtained YPO_4 hollow spheres were annealed at 750 °C for 2 h to determine the composition of the product. As shown from Figure 6b, no other diffraction peaks were observed except for the diffraction peaks from YPO_4. The results indicate that the pure YPO_4 phase was obtained after acid erosion.

Figure 7a is a low-magnification SEM image of the as-prepared sample after acid erosion. It indicates that the product is composed of a large quantity of microspheres. They greatly retain the uniform spherical structure after the process of acid erosion, and few were broken down. When these microspheres were strongly stirred in solution, the crushed particles were generated, revealing that the microspheres were hollow structures (see Figure S1c in the Supporting Information). The obtained microspheres have a diameter distribution ranging from 450 to 550 nm with an average diameter of nearly 500 nm. To clearly verify the hollow structure of the microspheres, transmission electron microscopy (TEM) was performed. The strong contrast between the dark edges and the pale center further confirms that all of the spherical particles have a large hollow cavity of about 400−500 nm in size and a shell thickness of 20−30 nm. The SAED pattern (inset in Figure 7) shows the diffraction ring pattern, confirming the polycrystalline nature of $YPO_4:Eu^{3+}$ hierarchical hollow spheres.

3.3. Mechanism for the Formation of the $YPO_4:Eu^{3+}$ Hollow Spheres. On the basis of all of the above experiment results, a general schematic illustration of the formation process of the YPO_4 hollow spheres was proposed in Figure 8. First, monodisperse colloid spheres of the $Y(OH)CO_3:Eu^{3+}$ were synthesized via urea-based

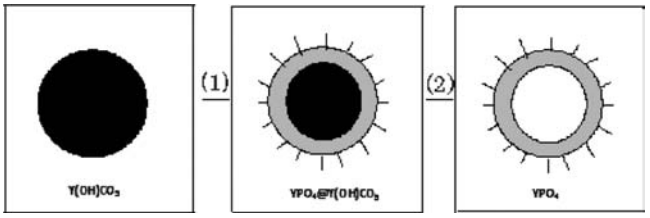

Figure 8. Schematic illustration of the formation process of YPO_4 hollow submicrometer-sized spheres: (1) hydrothermal process and (2) acid erosion.

homogeneous precipitation, which acted as the sacrificial template. In the following hydrothermal process, they partly reacted with $NH_4H_2PO_4$ to form a $YPO_4:Eu^{3+}@Y(OH)CO_3:Eu^{3+}$ core−shell structure. This process can be described as follows: At the initial stage of the reaction, there were several Y^{3+} ions ionized from $Y(OH)CO_3$ that were located around the surface of the $Y(OH)CO_3$ spheres. They reacted with PO_4^{3-} in the solution to form YPO_4 belts. Then, the $Y(OH)CO_3$ spheres were covered with a very thin layer of YPO_4. The just-forming shell was porous at the first stage, and the interior void between YPO_4 and $Y(OH)CO_3$ was filled with some amount of PO_4^{3-} ions. The PO_4^{3-} ions reacted with the interior Y^{3+} ions ionized from the $Y(OH)CO_3$ spheres to create the second layer of YPO_4, and so on. With the reaction proceeding, the outside shell of YPO_4 was gradually formed. Under these conditions, normal solution transport would appear to be the predominant shell-growth process.[20] As a few PO_4^{3-} ions could be transported through the forming shell of YPO_4, the $Y(OH)CO_3$ spheres were partly consumed to obtain the $YPO_4:Eu^{3+}@Y(OH)CO_3:Eu^{3+}$ core−shell structure after the hydrothermal process ran for 15 h, as shown from the TEM image of Figure 3c. Since $Y(OH)CO_3$ can be easily dissolved in the acid solution and YPO_4 is inactive, when the remaining $Y(OH)CO_3:Eu^{3+}$ was treated by nitric acid in the last erosion process, the YPO_4 hollow spheres were obtained as shown in Figure 7. In fact, the hollow sphere of YPO_4 could not be obtained in the one-step hydrothermal process over a long reaction time of 120 h (see Figure S2 in the Supporting Information), and the acid erosion process is necessary for the targeted product. In principle, our synthesis strategy might be extended to prepare the hollow spheres of other rare earth orthophosphates, such as $EuPO_4$, $GdPO_4$, $TbPO_4$, and $LuPO_4$, through their relatively colloid spheres in the sacrificial method.

3.4. Photoluminescence. Figure 9 displays the excitation and emission spectra of the $YPO_4:Eu^{3+}$ hollow spheres. The excitation spectrum consists of a strong broad band centered at 227 nm and a group of shape lines. The strong broad band is due to the oxygen-to-europium charge transfer band (CTB), and the sharp lines are assigned to the f−f transitions within the Eu^{3+} $4f^6$ electron configuration.[28] The maximum absorption line at about 397 nm is attributed to the $^7F_0 \rightarrow {}^5L_6$ transition of the Eu^{3+} ions. In the emission spectra, there are sharp lines ranging from 560 to 730 nm, which are associated with the transitions from the excited $^5D_0$ level to the ^7F_J ($J = 0, 1, 2, 3, 4$)

(28) Yu, L. X.; Song, H. W.; Lu, S. Z.; Liu, Z. X.; Yang, L. M.; Kong, X. G. *J. Phys. Chem. B* **2004**, *108*, 16697.

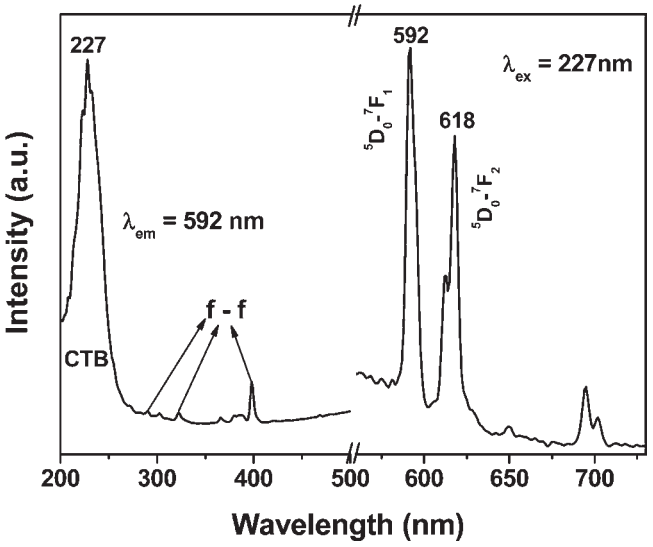

Figure 9. Room-temperature PL excitation and emission spectra of $YPO_4:Eu^{3+}$ hollow spheres.

levels of the Eu^{3+} ions. The major emissions around 592 nm ($^5D_0-^7F_1$) and 618 nm ($^5D_0-^7F_2$) correspond to the orange-red and red colors, respectively. In general, the Eu^{3+} ions can be used as a probe for the crystal field environments through comparison of the intensity of the $^5D_0 \rightarrow {}^7F_1$ (590 nm) transition with that of the $^5D_0 \rightarrow {}^7F_2$ (615 nm) transition. If Eu^{3+} is in an inversion center, the magnetic dipole transition is dominant, while in a site without inversion symmetry, the $^5D_0 \rightarrow {}^7F_2$ electronic transition becomes the strongest one. Therefore, the strongest emission of the $^5D_0 \rightarrow {}^7F_1$ transition indicates that the Eu^{3+} ions locate at the sites of inversion symmetry in the YPO_4 host matrix. The luminescence of the as-prepared $YPO_4:Eu^{3+}$ sample coupled with their hollow structure may have potential applications in biological fields.

4. Conclusions

We have developed a facile method to synthesize submicrometer-sized $YPO_4:Eu^{3+}@Y(OH)CO_3:Eu^{3+}$ core–shell structures and $YPO_4:Eu^{3+}$ hollow spheres via the colloidal spheres of $Y(OH)CO_3:Eu^{3+}$ acting as reaction precursors as well as the template. The whole process mainly consists of the hydrothermal reaction and the following acid erosion. The submicrometer-sized $YPO_4:Eu^{3+}$ hollow spheres are uniform with a shell of about 20 nm in thickness. Due to the high chemical stability and luminescence functionality, the obtained $YPO_4:Eu^{3+}$ hollow spheres may have potential applications in drug release, as well as cell biology and diagnosis.

Acknowledgment. This work is financially supported by the National Natural Science Foundation of China (Grant No. 20771098), the Fund for Creative Research Groups (Grant No. 20921002), and the National Basic Research Program of China (973 Program, Grant Nos. 2007CB935502 and 2006CB601103).

Supporting Information Available: The low-magnification SEM images of the crushed particles generated by the hollow sphere after stirring (Figure S1); the SEM image of hollow sphere 120 h after acid erosion (Figure S2). This material is available free of charge via the Internet at http://pubs.acs.org.